ORIGINAL
12/10/97 B

Insulating Biomaterials
N01-NS-62350

Fourth Quarterly Progress Report
July-September, 1997

Submitted to:

Neural Prosthesis Program
National Institutes of Health
National Institute of Neurological
Disorders and Stroke

By the:

Biomedical Microelectronics Laboratory
Biomedical Engineering Center, Massachusetts Institute of Technology
West Roxbury VA Medical Center

Contributors:

David J. Edell, PI
Karen K. Gleason, Chemical Engineering
Bruce C. Larson, Grad Student, Electrical Engineering
Scott Limb, Grad Student, Chemical Engineering
James R. Mann, Electrical Engineering
Terry Herndon
Sean Sexton, Electronics
Cynthia M. Vanaria, Assembly

Introduction

We are making good progress on the animal implant instrumentation issues, Kapton ribbons, chip surface coatings, multi-temperature multichannel electrometer system, etc. However, only two aspects of this work will be summarized this quarter - silicones for encapsulation of the bond area of silicon devices, and vapor deposited silicone development. A draft of a paper has been appended which summarizes our work on encapsulation of the bond area. A summary of vapor deposited silicones follows here.

Pyrolytic chemical vapor deposition of poly(organosiloxane) thin films

Summary:

A pyrolytic chemical vapor deposition method was used to deposit silicone polymer thin films from the thermal decomposition of the cyclic tetramer, octamethylcyclo-tetrasiloxane, over a hot-filament. High deposition rates (up to 2.5 μm/min) could be achieved. Fourier transform infrared spectroscopy verified that the deposited films had the same functional groups as a poly(dimethylsiloxane) standard, though with a measurably lower methyl concentration. X-ray photoelectron spectroscopy showed that a typical film had an elemental composition of C:Si:O / 1.5:1:1, confirming the loss of methyl groups. The dependence of the growth rate on the filament temperature gave an apparent activation energy of 36.5 ± 4.1 kcal/mol.

Description

Silicone is a generic name for the class of polymers which consist of a repeating Si-O backbone with organic functional groups attached to the Si via Si-C bonds. The most common of these functional groups is methyl, resulting in the silicone, poly(dimethylsiloxane) or PDMS. Because of its excellent combination of properties, conventional crosslinked PDMS is used in a wide range of applications from the potting and encapsulation of electronics and electrical connections to medical implants such as heart valve poppets and intraocular lenses. There has been considerable interest in extending these applications through the chemical vapor deposition of silicone thin films. To date, all such efforts have focused on plasma enhanced CVD (PECVD) deposited films from a large variety of monomers such as hexamethyldisiloxane, tetramethylsilane, and octamethylcyclotetrasiloxane. A potential problem in the application of these films as dielectric layers, however, arises due to the high dielectric loss when compared to the conventional polymer as well as an aging effect upon exposure to the atmosphere. Both of these effects can be related to the high density of trapped radicals in plasma deposited materials. These defects can originate from electron impact fragmentation of gaseous reactants and from UV irradiation ion bombardment of the surface. A pyrolytic process, on the other hand, in which the growth precursors are thermally produced does not suffer from ion bombardment and

UV irradiation and has been shown in the case of fluorocarbon polymer CVD to result in a lower density of dangling bonds.

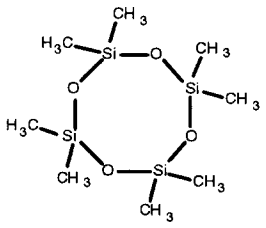

Figure 1: octamethylcyclotetrasiloxane

We have demonstrated a pyrolytic process for the deposition of silicone thin films from the low-pressure thermolysis of octamethyl-cyclotetrasiloxane, $[(CH_3)_2SiO]_4$, also known as D_4 from the commonly used nomenclature of D for $-(CH_3)_2SiO-$. D_4 is a monomer which is commonly used in the base catalyzed, liquid phase ring-opening polymerization to PDMS. In addition, D_4 melts at 17 °C and hence is a liquid at standard conditions with a reasonable vapor pressure.

In our experiments, approximately 2 sccm of D_4 was vaporized through the reactor chamber (Figure 1) by mildly heating a Pyrex container attached to a valve on the chamber. Pressure was maintained at 0.6 torr by adjusting a throttle valve in the reactor outlet. A 1 mm diameter tantalum wire was resistively heated to between 260 and 530 °C for these experiments. The substrate was a 2" Si wafer sitting 11 mm away on a water cooled stage; the temperature as measured by a thermocouple on the backside of the wafer was 20 ± 3 °C. The growth rate in the center of the substrate varied from 2.5×10^4 to 5 Å/min depending on the filament temperature. By comparison, the maximum deposition rates reported for the plasma polymerization of hexamethyl-disiloxane varied from 0.5 $\mu g\ cm^{-2}\ s^{-1}$ for capacitively coupled discharges to 2.6 $\mu g\ cm^{-2}\ s^{-1}$ for microwave discharges, which translates to linear growth rates of about 3×10^3 and 1.6×10^4 Å/min, respectively.

A comparison of the typical Fourier transform infrared spectra of a CVD thin film produced at a filament temperature ($T_{filament}$) of 415 ± 5 °C versus that for a viscous liquid PDMS standard (Aldrich Chemical, secondary standard) is shown in Figure 2. A qualitative analysis of the spectra indicates that the sample and the standard have absorbance peaks at identical wavelengths and hence identical IR active functional groups. In order to permit semi-quantitative analysis, the spectra are shown in normalized absorbance units. The main feature to note in this case is the marked difference in relative intensity between the CVD film and the standard at 2964 cm^{-1}, 1410 cm^{-1}, and 702 cm^{-1}. The peaks at 2964 cm^{-1} and 2906 cm^{-1} are due to the asymmetric and symmetric C-H methyl stretches, respectively, while the peak at 1410 cm^{-1} is the result of the C-H methyl bending modes. This implies that the CVD film is deficient in methyl substituents as compared to the PDMS standard. We can also rule out the loss of sp^3-CH_3 absorption intensity due to any C-C crosslinking since such a rearrangement would result in the appearance of new peaks in the C-H stretch region at a lower wavenumber corresponding to sp^3-CH_2. The peak at 702 cm^{-1} is in a region which is typically assigned to Si-C stretches.

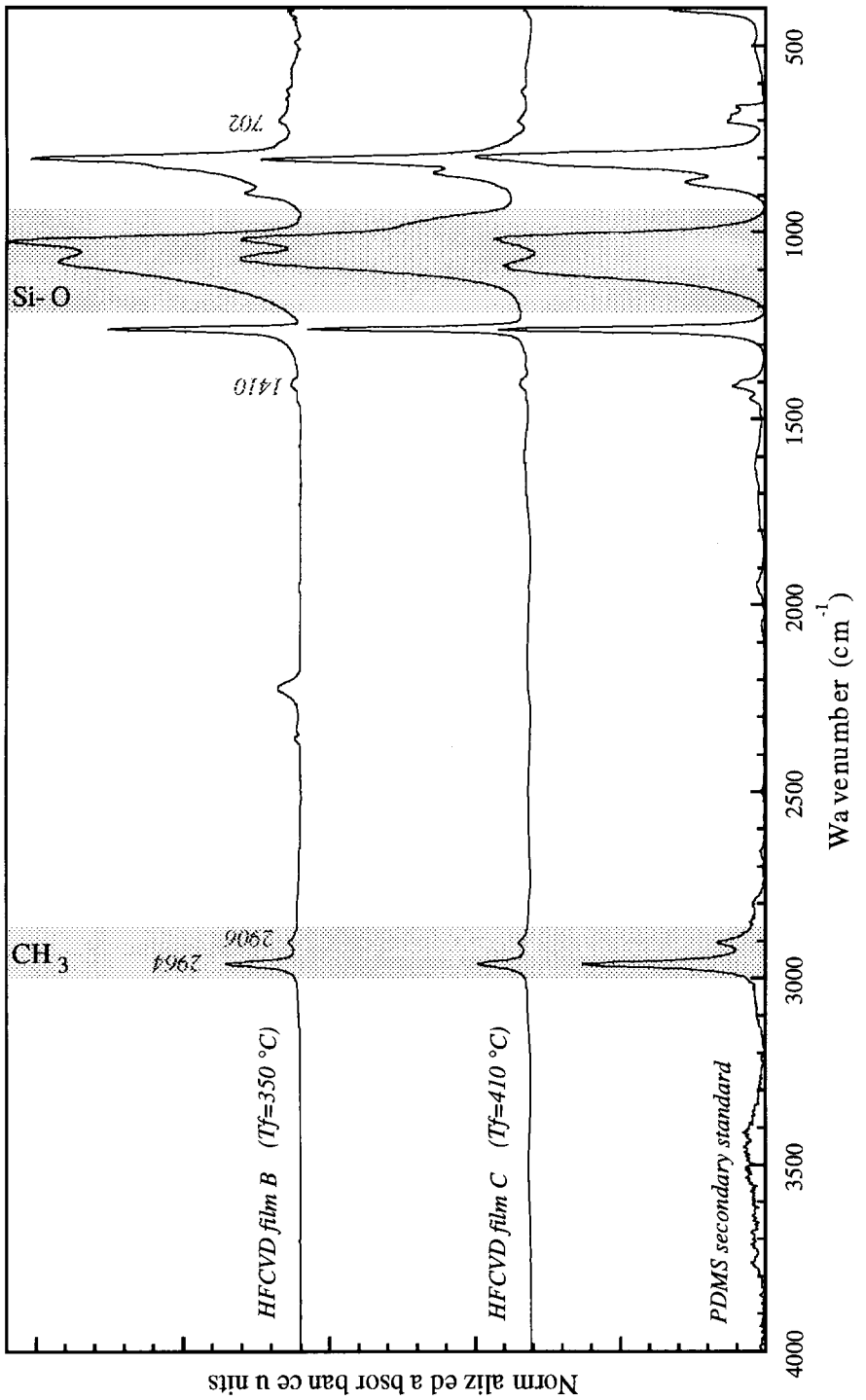

Figure 2: Comparison of FTIR spectra of a 6.9 µm thick pyrolytic CVD thin film with a poly(dimethylsiloxane) standard

Further analysis was carried out by X-ray photoelectron spectroscopy (XPS). Survey scans were conducted on several CVD thin films as well as the PDMS standard

to determine the relative elemental composition. By assuming that the PDMS standard has the ideal elemental composition of C_2SiO and adjusting the instrument sensitivity factors for the O 1s, C1s, and Si 2p peaks to reflect this, the composition of the $T_{filament}$ = 415 °C sample was determined to be $C_{1.53}Si_{1.00}O_{1.00}$ which confirms the loss of methyl substituents shown by FTIR spectroscopy. It further shows that the Si-O backbone is left intact by the deposition process. The films deposited at other filament temperatures demonstrated similar compositions. The loss of methyl groups may lead to crosslinking in the films. To test this hypothesis, solubility tests on as deposited thin films were conducted in benzene, toluene, and a mixture of xylene isomers. In all cases, the weight loss was minimal, being less than 10% and limited by the resolution and accuracy of the balance.

In order to better understand the kinetics of this process, the growth rate was measured at several filament temperatures and the results plotted in Arrhenius form. For films under approximately a micron in thickness, the deposition rate was measured by ellipsometry. Thicker films were measured by scratching the film and using a stylus profilometer. Figure 3 is a graph of the natural log of the growth rate versus the reciprocal of the filament temperature. A linear fit to the data is shown and yields an activation energy of 36.5 ± 4 kcal/mol.

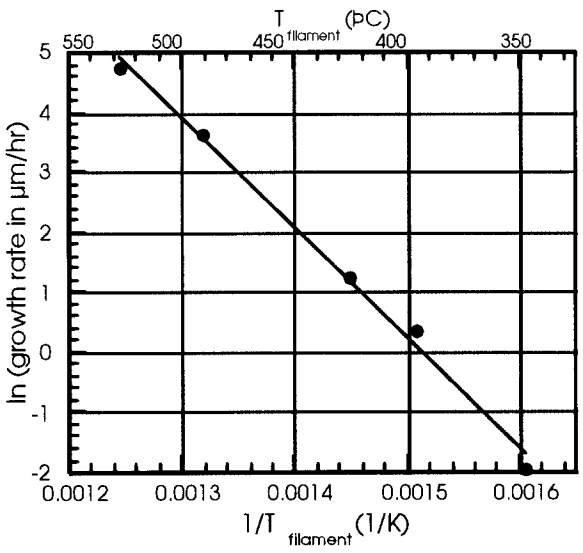

Figure 3: Arrhenius plot for pyrolytic CVD at 0.6 torr

A thermally activated process for the CVD of silicone-like films, which have a similar structure to that of poly(dimethylsiloxane) as confirmed by FTIR spectroscopy, has been demonstrated. In contrast to PECVD, the pyrolytic CVD process does not involve any ion bombardment or UV irradiation thus eliminating the possibility of related atomic rearrangements and defects. The ability to grow fluorocarbon and silicone thin

films by pyrolytic CVD reveals that ion bombardment, which is often cited in discussions of PECVD mechanisms as being essential to the creation of active sites for film growth, is in fact not necessary for the deposition of these materials. In addition, very high silicone growth rates have been achieved by pyrolytic CVD. We anticipate that changes in reactor conditions such as pressure, filament-to-substrate standoff, flow rate, and substrate temperature will result in even higher rates.

Introduction

One of the chief concerns for implantable microelectronic devices is the hostile environment of the body. Some implantable microelectronics such as those used for pacemakers and cochlear prostheses can be sealed in titanium canisters to protect them from the biological environment. Other applications of implantable microelectronics include devices that can interface with the nervous system for neuroprosthetic applications in rehabilitation. Such neural interface devices are being developed which will be attached and embedded in neural tissue. These devices must be many times smaller than pacemakers or cochlear implants to minimize damage to target neural structures during placement and to allow devices to fit into small spaces without damaging adjacent tissue. In addition, neural interface devices must be biocompatible and bioresistant. Biocompatibility is essential to minimize formation of connective tissue between neurons and electrode contacts over the course of long term implantation. Bioresistance is essential to ensure that the implanted electronic device remains functional for many decades.

Devices approaching these ideals are being developed at a variety of locations worldwide using micromachining of silicon as a primary tool [1-11]. There is also a National Center for Research Resources funded National Resource Center located at the University of Michigan which both develops and supplies micromachined silicon devices for neurophysiology.

Silicon may be a good choice of materials since silicon technology is highly developed. Of perhaps greater significance, silicon naturally forms an inert, self limiting oxide that is biocompatible [2, 3]. Micromachining can be used to produce a variety of novel structures that may approximate the ideal neuroprosthesis using this technology. However, as fabricated, micro-machined devices typically are not bioresistant. Figure 1 illustrates some possible failure modes when an integrated circuit micro-device is immersed in saline environments for extended periods of time.

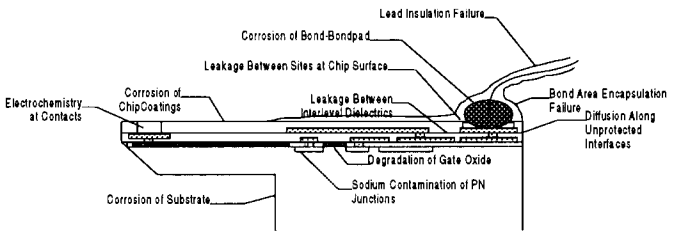

Figure 1: *Sketch of some failure possibilities for integrated circuit micro-devices.*

There are several problem areas associated with operation of micro-fabricated electrical devices within physiological systems:

1. The wires used to attach to the device must be capable of withstanding immersion in ionic fluids with a 5 volt magnitude bias across the insulation.

2. The exposed areas where the wires are attached to connectors or devices must be coated with a material that is typically applied after bonding has been accomplished.

3. If microribbon cable technology is used, it is necessary create a void free seal in the area under the microribbon where it attaches to the device.

4. The wire assembly must be flexible enough to minimize static forces applied by the implanted element on the tissue. Dynamic flexing is unlikely to be a problem in the protected areas where the devices are to be used.

5. The circuits on the chip must be protected from water and ionic contamination (i.e. the surface density of sodium ions in the MOS gates should be less than $10^9/cm^2$).

6. The chip surface materials, the chip substrate, and encapsulants must all be bioresistant.

While silicon integrated circuit technology is highly developed, materials used successfully by the electronics industry for protecting integrated circuits are not necessarily compatible with the saline environment of biological systems. This fact is often unappreciated. Several examples exist of unexpected failures from materials that were not tested under realistic conditions. One example was the extensive use and proposed use of polyimide for development of neuroprostheses. This choice was based on the experience of the electronics industry, but the material had never been fully evaluated under saline conditions. However, since 1971 it has been known that polyimide is susceptible to hydrolysis [12]. Parylene has been widely promoted as an insulating biomaterial. While effective for short term encapsulation, upon exposure to high humidity, Parylene undergoes hydrolysis with resultant craze cracking [13].

Development of materials and processes for fabrication of bioresistant integrated circuits has been the focus of recent work sponsored by NIH [14]. The goal of studying the bioresistance of micro-electronic devices is to develop new packaging techniques that minimize volume and maximize long term reliability. This report focuses on one aspect of this ongoing research – insulation and protection of the bond area of micromachined neural probes.

Accelerated testing is being approached from three perspectives: high sensitivity detection of degradation; overstress testing; and physical properties observations. The most useful for this work has been high sensitivity test devices and measurement instrumentation. By detecting subtle changes in device parameters many orders of magnitude below where overt device failure would be expected, it may be possible to determine possible long term failure. Overstress testing is being used to detect subtle changes in device parameters during overstress acceleration of possible failure modes. This may yield clues for reliability assessment earlier than high sensitivity detection alone. However, over-stress testing may lead to erroneous conclusions if a complex aging process is involved. Monitoring of chemical and mechanical properties may give clues to possible long term failure modes even though other tests give no indication of degradation. For example, the mechanical properties of an insulator may change radically with no electrically measurable changes. At some point, the film may develop cracks causing unanticipated, catastrophic failure similar to the problematic pacemaker leads and kapton flex-circuits. This report focuses on use of high sensitive tests for evaluation of the long term reliability of encapsulant-silicon dioxide interfaces.

Methods

The general approach taken in this long term research was as follows:

1. Develop sensitive test structures and appropriate assembly techniques.
2. Develop sensitive testing techniques.
3. Evaluate a variety of candidate materials.
4. Identify classes of materials with potential for this application.
5. Develop new materials in these classes with perhaps better properties.

It is important to keep in mind that the following results should be considered as an interim report on one aspect of progress in this long term research program.

Test Structures

Appropriate test structures for evaluation of surface leakage currents should be constructed of materials relevant to the micromachined neural interface devices. Usually, thin film dielectrics such as silicon dioxide and silicon nitride will be used to insulate interconnects to minimize bulk and allow devices to be inserted into neural tissue. The bond area of integrated circuits usually consists of exposed surfaces of metals surrounded by exposed surfaces of silicon dioxide. Often, silicon nitride coatings are utilized to protect underlying circuits from water and ionic contamination. When silicon nitride is exposed to moisture or oxygen, the surface gradually oxidizes to form silicon dioxide. It therefore seemed reasonable to construct test devices with silicon dioxide surfaces for evaluation of encapsulants for the bond pad area. A variety of metals can be used to form conductors on micromachined silicon devices. In order to obtain a sensitive test for long term evaluation of encapsulants, it was decided to use a noble metal so anodic oxidation of the traces would not artificially limit leakage currents. Initially, gold was chosen for ease of fabrication and bondability. However, after the first assemblies were completed, it was apparent that regardless of how carefully the processing was accomplished, surface resistivity was limited to $10^{6\text{-}9}\Omega/\bullet$ rather than the anticipated $10^{12\text{-}18}\ \Omega/\bullet$. New structures were fabricated using platinum which yielded surface resistivity on the order of $10^{15}\ \Omega/\bullet$. Two designs of test devices were fabricated and used to evaluate surface encapsulants.

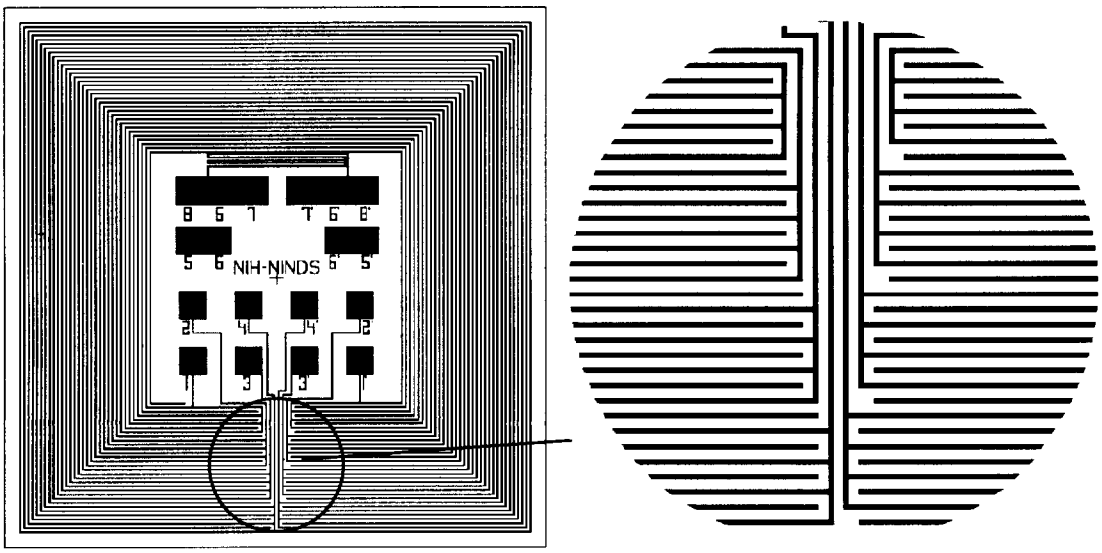

Figure 2: LEFT: Bond Chip design. Overall size was 4mm square. RIGHT: Portion of pattern for IDE bond chip showing four sets of IDE traces arranged from the outside of the chip to the inside. Traces were 10μm wide separated by 20μm spaces.

Bond Chip Design

"Bond chip" devices were designed to evaluate leakage currents between isolated metal conductors at the interface between the encapsulation and the chip surface. Such leakage

currents could result in electrolysis of the metal traces and formation of dendrites that may eventually lead to short circuiting of the conductors. In order to maximize the probability that conductive pathways will be observable, the length of the edges of the conductors should be maximized and the distance between conductors should be minimized. In addition, the width of the conductors should be minimized to reduce volume conduction currents that will flow in parallel with surface leakage currents. One appropriate conductor pattern is the InterDigitated Electrode (IDE) pattern as shown in Figure 2. This bond chip was designed with four concentric sets of IDE pairs which allows detection of failure modes that propagate from the outside edge of the encapsulation inward or from the bond area outward. The traces were 10μm wide separated by 20μm spaces. By applying a voltage to one set of electrodes and then measuring currents through other electrodes, the resistance of the chip-encapsulation interface could be assessed. Since the actual surface resistance measured is a function of the length of the parallel electrodes and the electrode separation, it was convenient to normalize the measurement by expressing it as ohms/square (Ω/•). A square is formed by a length of electrode equal to the separation width. The total number of squares is equal to the total length of the electrode edges divided by the separation width. Since leakage currents of interest are expected to flow across the separation between electrodes, dividing the measured resistance by the total number of squares between conductors yields a normalized measurement with units of ohms/square. The number of squares for these devices ranged from $2x10^{-4}$ for the outer electrode pair to $3.7x10^{-4}$ for the inner electrode pair.

In addition to assessing the surface resistivity of the encapsulant-chip system, the bond chip also allows assessment of bond wire to bond pad resistance, bond pad to contact resistance, and polysilicon resistor resistance. These measurements are accomplished by four point technique where sensing connections are used to measure the voltage at the device across the resistance of interest. For example, to measure the bond resistance the bond wire is double bonded – first to a voltage sensing electrode and then to a current return and voltage sensing electrode. By applying a current to the wire and measuring the voltage drop across the bond, the resistance can be computed. Similar arrangements are used for measuring the contact and polysilicon resistances.

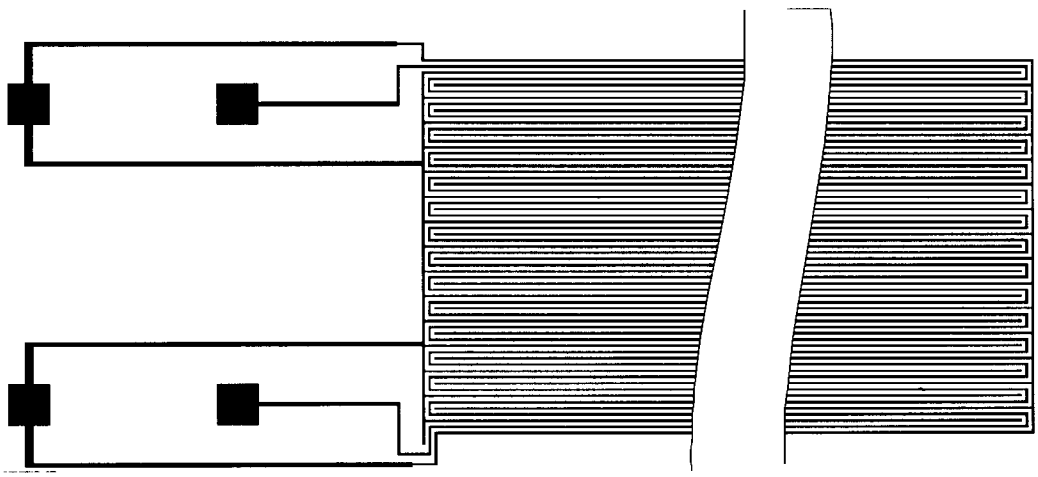

Figure 3: Triple Track design where measurements are taken by applying voltage to outer electrodes and measuring current on inner electrode. The overall length of the device was 1.2cm and the width was 2mm. There were $3x10^{-5}$ squares of surface resistance.

One of the problems associated with using the Bond Chip design was that the bonding process occurred close to the IDE sensors. While this might be thought of as a practical test, in fact in a research laboratory it is very difficult to achieve the level of cleanliness necessary for particulate free bonding of the 16 connections used for this assembly. Another problem associated with Bond Chips was the lack of a direct measure of continuity of the connections. This was intentional in order to minimize stray leakage baths from interconnects, connectors and relays used in the measurement system. While the continuity could be inferred from capacitance measurements between the electrodes and the substrate, such measurements are indirect and can be unreliable.

Triple Track Design

After several years of experience with using Bond Chips, triple track devices were designed to improve measurement sensitivity and reliability. While Bond Chips yielded useful data, bond area contamination during assembly was a chronic problem. Triple Track devices were designed to have bond pads distant to the IDE pattern. Bond pads were at least 175μm from the nearest trace and 800μm from the triple track sensor. This allowed some local contamination of the bond area to occur without compromising the measurements because defects created by the contamination were seldom large enough to bridge two traces. Four bond pads were included for each triple track device to allow direct assessment of continuity.

Assembly Procedures

All polymeric encapsulants transport water molecules. While some polymers transport water more slowly than others, since the volume of the interface is small, the encapsulant-interface system can be considered at equilibrium after a relatively short time under soak. Materials at the interface will be fully hydrated. Thus contaminants on the surface of the implantable devices can drastically alter the behavior of the device under soak. Another important principle of assembly for implantable devices is that the outer layer of atoms on the surface of a device determines the chemistry of the bonds between the encapsulant and the interface. If a silicon dioxide surface is coated with a monolayer of hydrocarbons, then the critical bonds will be between the hydrocarbons and the surface, and the hydrocarbons and the encapsulant. Thus the soak test will demonstrate the behavior of a three layer system rather than the behavior of the encapsulant-silicon dioxide system.

While these devices had been previously fabricated in a clean room and stored in a relatively clean environment, over time contaminants can accumulate on the surfaces. This was initially observed by noting that clean, hydrophilic silicon devices that had been stored for more than a few weeks became markedly hydrophobic indicating that the surface had become contaminated. A three part cleaning procedure was developed for biomedical implantable silicon devices – solvent, chemical oxidation, and ultra-violet/ozone exposure.

Solvent cleans consisted of serial rinses in acetone, isopropyl alcohol, deionized water, isopropyl alcohol. Ultrasonic agitation and microscopic examinations were often combined with the last isopropyl step to remove adherent particles. Solvent cleaning alone was not always successful in restoring the hydrophilic surface.

A highly oxidizing cleaning solution can remove most of the contamination by destroying the hydrocarbons. Boiling, concentrated nitric acid and concentrated hydrogen peroxide mixed 2:1

is one aggressive cleaning step that can remove most or all hydrocarbon contamination of the surface. Another aggressive and perhaps more convenient oxidation cleaning step is to use a 2:1 mixture of concentrated sulfuric acid and concentrated hydrogen peroxide. The fresh-mixed solution self heats to 100-150^{0}C and vigorously attacks any exposed hydrocarbon material. Following chemical oxidation, the devices must be rinsed and dried before coating. Typically this was accomplished by rinsing in de-ionized water to remove acid residuals followed by isopropyl alcohol to remove water residuals. It was not clear that an atomic layer of hydrocarbon contamination did not still persist after the bulk of the hydrocarbons had been removed from the surface by chemical oxidation.

UltraViolet-Ozone (UV-O) has been shown to remove chemically bonded hydrocarbon contamination of a silicon dioxide surface. UV-O reactors generate intense fields of ultra-violet light using mercury lamps. Oxygen in the air is converted to ozone. When a sample surface is placed close to the UV-O source, ultra-violet rays can activate the atoms on the surface and the intense ozone environment can oxidize the hydrocarbons. The resulting surface is likely pure silicon dioxide, suitable for evaluation of encapsulants.

Coatings must be applied as soon as practical after the final UV-O cleaning step to minimize re-contamination of the surface. By coating the IDE areas of the test devices first, contamination during bonding and final assembly was minimized.

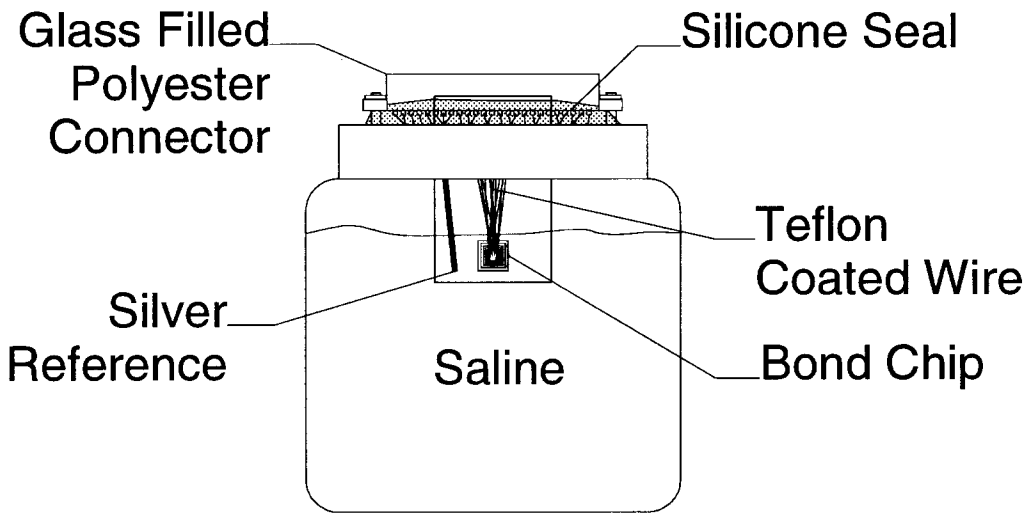

Figure 4: Test assembly for Bond Chip. Approximately 0.01% silver nitrate was added to the physiological saline for bacteriostasis.

At the beginning of this research, it was not clear what insulating materials would survive long term saline soaks. Thus choices for insulation of the bond wires were based on prior experiences with implantable devices. At the outset of this research, it was thought that epoxy based encapsulants were the most likely to retain insulating properties during long term saline immersion [15], and hence epoxies were used as the default insulator over wires and connectors. Also, from prior experience with implantable devices, Teflon® insulation appeared to hold up for long term use in saline environments. Silicones had also been used on the implantable devices, but at the time it was thought that silicones were biocompatible materials that weren't particularly good for insulation because they readily transported water vapor. Since the soak tests were to proceed for many years, it was essential that appropriate materials be selected.

Otherwise, if the wire or connector insulation failed, it would be impossible to further evaluate the chip surface encapsulation. Subsequent results from long term testing of wire insulation and silicone chip surface encapsulants showed that both of these materials provided outstanding insulation performance over long times. Epoxies, on the other hand, often failed by shrinkage or fracture after long term soaks. Later in the study Teflon® insulated wires overpotted with silicone were relied upon for connecting the bond chips and triple tracks to the connectors. **Figure 4** shows the assembled test jar. Glass filled polyester connectors were selected after extensive testing to find connectors that would maintain $10^{15}\Omega$ resistance indefinitely. A silver wire in the solution provided ground reference. Once the assemblies were completed, they were first tested dry and then filled with physiological saline with 0.01% silver nitrate for bacteriostasis.

Instrumentation and Measurements

An automated measurement system was developed to allow accurate measurements of resistances greater than $10^{15}\Omega$. A Keithley 617 electrometer was used to detect currents from 10^{-3}A to 10^{-14}A. A computer system switched between pairs of IDEs and acquired data from the electrometer. Typically, measurements consisted of stepping voltages between ±5volts at 1 volt increments, allowing the electrical transients to settle until there was no detectable drift of the reading, and then acquiring 100 readings for averaging. At the completion of the IV sweep, linear regression was used to fit a line to the resulting data set for computation of the resistance.

Bond to pad resistance, pad to polysilicon contact resistance, and polysilicon resistances were also measured using four point techniques. Current sweeps were injected through the structure via one set of connections and measuring the voltages developed across the devices using high input impedance instrumentation amplifiers. Linear regressions were used to compute the resistances.

Selection of materials to be tested

In the beginning of this research it was not known what materials should be used for protection of the bond area. It was known that epoxies were relatively long lasting materials that were chemically resistant, and they were being extensively used by the electronics industry. Some materials such as polyimide, parylene, polyurethane, and formvar were excluded because they failed long term soak testing as wire insulations [15]. Other materials such as Teflon®, polyesterimide, polyethylene, etc. were difficult to process for this application. Silicones were considered because they had been used as biocompatible overcoats of bond areas that had been protected with epoxies in prior work [16, 17]. The influence of silicone encapsulants on the survival of the epoxy was of interest. All epoxy coatings failed after a few weeks immersion in saline solutions. While the initial readings were $10^{15}\Omega/\bullet$, after a few days to a few weeks under soak at 37°C, the epoxy-silicon dioxide bonds delaminated. The silicone encapsulated surface, however, survived much longer. Thus, silicones were aggressively explored as bond area encapsulants. In 1988, Dow Corning Corporation was the largest supplier of silicones for medical and electronics applications. Dow Corning was intensely involved in development of silicone encapsulants and supplied several experimental formulations. After Dow Corning Medical was sued over breast implant issues, Dow Corning no longer allows their products to be used for long term implants. Other suppliers of silicones were contacted and replacement

materials for the Dow Corning silicones were identified and put under test. However, the experimental silicones supplied by Dow Corning were proprietary and could not be duplicated.

Results

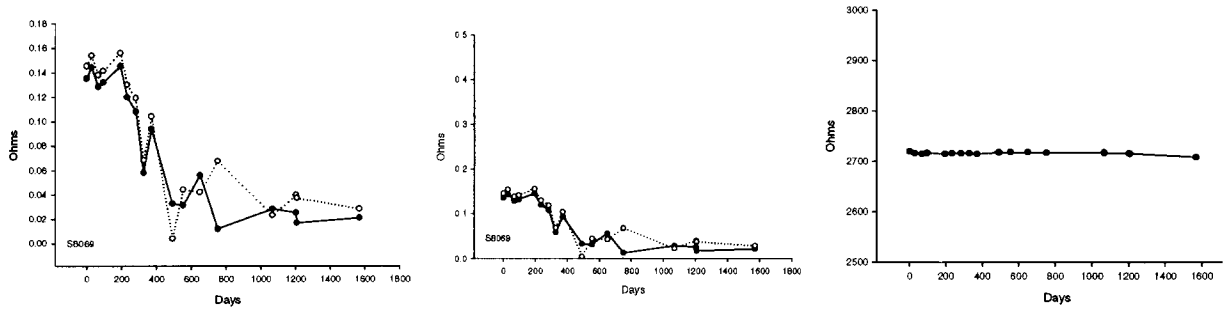

Figure 5: Long term measurements of resistor structures on Bond Chip S8069W01 encapsulated with Dow Corning x8069 silicone. Left plot is for two bond-bond pad resistance structures. Middle plot is for two platinum-polysilicon contacts. Right plot is for polysilicon resistor.

Examples of long term four point measurements of bond resistance, contact resistance and polysilicon resistor resistance are shown in Figure 5. After about one and one-half years, the resistances of the bonds and contacts had fallen by a factor of 10 or so and leveled off. Polysilicon resistance was remarkably stable for about 4 years. Recently it appears that there may be a gradual reduction in measured polysilicon resistance. Most devices show relatively stable bond, contact and polysilicon resistances unless delamination of the encapsulant occurred as noted in the results below.

An example of a voltage/current (V/I) sweep for an IDE pair encapsulated with Dow Corning x8069 silicone is shown in Figure 6. Each data point is the average of 100 samples taken after electrical transients caused by incrementing the voltage have dissipated. The slight loop is caused by residual transient charge injected by the voltage steps. This resistance reading corresponds to an equivalent surface resistivity of $7x10^{18}\Omega/\bullet$. One confounding factor in these measurements is that the volume conduction of the encapsulant and the substrate surface insulation appear as parallel resistances to the surface conductivity. Thus these readings should be considered lower estimates of the true surface resistivity.

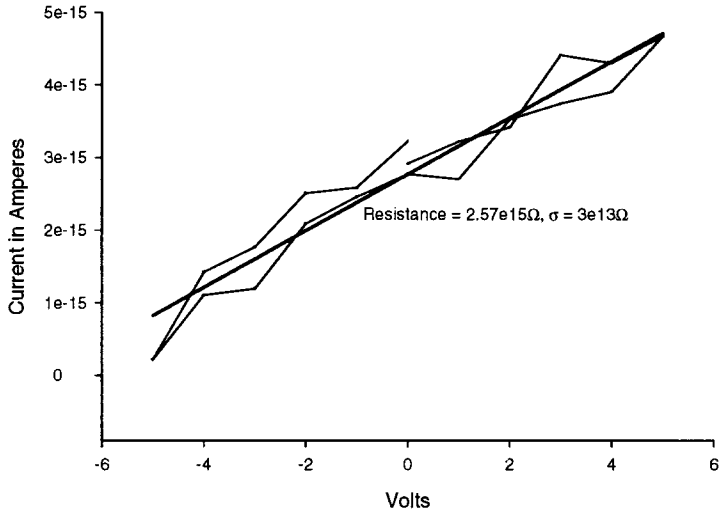

Figure 6: Single Voltage/Current sweep of electrode pair V03E04 which are located in the center of the bond chip. The bond chip was encapsulated with Dow Corning experimental silicone encapsulant x8069 six years previously. The straight line is a best fit linear regression analysis.

To assess the magnitude of the parasitics, measurements were taken between one electrode of an IDE set and another electrode from a different IDE set on the same substrate. Typically, for silicones, resistances between non-adjacent electrodes were an order of magnitude greater than the resistances measured between IDEs. Thus it could be inferred that the measured resistances were dominated by the resistance of the surface interface.

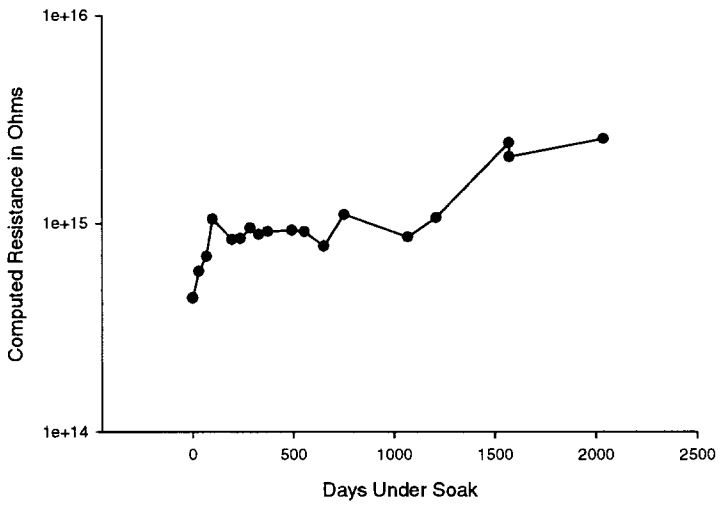

Figure 7: Long term resistance data from bond chip encapsulated with Dow Corning experimental silicone encapsulant x8069.

Figure 7 shows an example of a six year measurement for one IDE encapsulated with x8069. The slight rise in resistance with time is often observed with silicone encapsulants. At the same time, volume resistance decreased slightly indicating that the effect was due to an increase in surface resistivity rather than volume resistivity. Figure 8 shows summary data from eight years of measurements with a bond chip encapsulated with Dow Corning MDX-4-4210. This particular data set illustrates failure of Pair 1, the inner electrode set adjacent to the bond pads,

while the more peripheral electrode sets remain insulating for many years. These readings correspond to surface resistivities of approximately $3x10^{16}\Omega/\bullet$ which is typical for most silicones tested other than the experimental types.

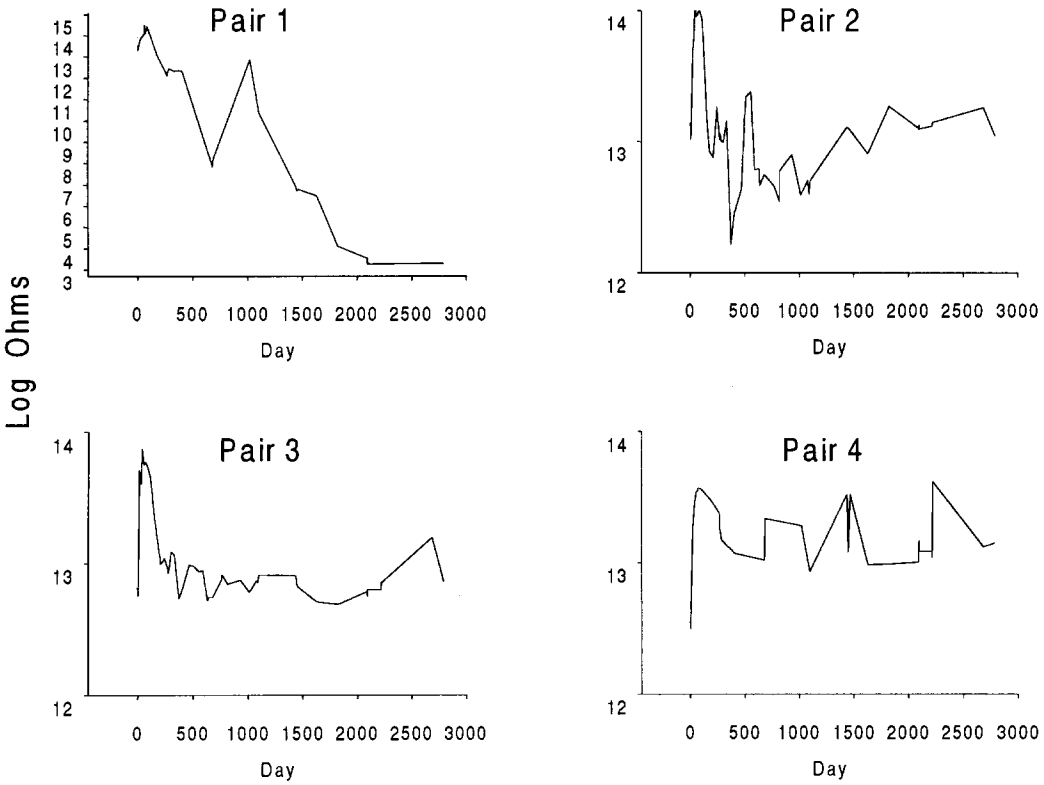

Figure 8: Summary of long term soak test results from bond chip encapsulated with Dow Corning MDX-4-4210 silicone elastomer. Graph Pair 1 is from inner ring of IDEs, closest to the bond pads and farthest from the edge. Pair 4 is from outer ring of IDEs, farthest from the bond pads and closest to the edge.

Table 1and Table 2 summarize results of successful encapsulations of Bond Chips and Triple Track devices. The tables are generally organized according to the material used to coat the devices, and whether or not UV-Ozone was used prior to encapsulation. UV-Ozone was a standard procedure in our lab for many years, but for a time after changing facilities and personnel, this step was inadvertently omitted. The first two devices listed (D4210T and D6863W01) were control devices where wires were left floating in the encapsualant over the pads. Most of the silicones tested were similar to Dow Corning MDX-4-4210 which was a fumed silica filled, platinum catalyzed, addition cure polydimethylsiloxane. The exceptions were a fluorosilicone elastomer (Nusil CF2-3521), a low viscosity coil impregnating silicone (Nusil R-2620), and three experimental "glob top" silicones (Dow Corning X-6863, X-6863B, X-8069). All of the MDX-4-4210 like silicones performed similarly, generally maintaining surface resistivities of greater than $10^{16}\Omega/\square$ for many years with a few exceptions listed in Table 4. The experimental "glob top" coatings provided excellent surface resistivities of greater than $10^{18}\Omega/\square$ for many years. While generally there were slightly more failed electrode pairs in the devices where the UV-Ozone step was omitted, other factors such as assembly inexperience causing recontamination of the surfaces or improper initial cleaning could also have accounted for this difference.

The devices that failed completely are listed in Table 3. There were 4 devices for a total of 16 IDE pairs that failed in 2.5-80 months after being encapsulated with MDX-4-4210. None of these devices were assembled without some deviation from normal assembly procedures. BGTSP425 was cured at 200°C overnight instead of the normal 3hr, 150°C cure that was standard for this material. G42103 was assembled without use of the UV-Ozone surface preparation step which may have left a slight surface residue that could interfere with bonding of the silicone to the surface. BGTSP426 was the first device to be assembled by an inexperienced technician in a new facility. CGTSP421 was assembled using Epoxy Technology H77 over the wiring which may have shrunk sufficiently during long term soak to lift the silicone and wires from the surface of the device.

R6100 and Sylgard-184 were designed for the electronics industry for potting of electronics assemblies but apparently lacked sufficient reactivity with silicon dioxide surfaces to be effective encapsulants for silicon chips.

Also shown in Table 3 are the epoxy results. Four epoxies using two types of curing systems – amine and anhydride – had been tested as possibly good encapsulants for this application. Epoxy coatings failed within a few days to weeks following immersion in saline solutions. When dry, all epoxies exhibited greater than $10^{19}\Omega/\square$ of surface resistivity. However, once immersed in saline, all failed within a few days to a few months. This data was collected from 8 epoxy encapsulated bond chip and triple track devices with a total of 32 IDE pairs

Device ID	Material	Manufacturer	Description
D4210T	MED-4210	NuSil Technology	Silicone elastomer (MDX44210 like), dummy wires embedded in silicone above TT pads.
D6863W01	X-6863B	Dow Corning	Filled silicone without carbon black dummy with wires embedded in silicone above pads.
BGTSP681	X-6863	Dow Corning	Filled silicone with carbon black bare edge assembly of bond chip design.
S6863W66	X-6863B	Dow Corning	Filled silicone without carbon black bare edge assembly of bond chip design.
S6863W02	X-6863B	Dow Corning	Filled silicone without carbon black bare edge assembly of bond chip design.
S8069W01	X-8069	Dow Corning	Filled silicone without adhesion additive found in X-6863 bare edge of bond chip design.
BGTSP421	MDX-4-4210	Dow Corning	Silicone elastomer, bare edge assembly of bond chip design.
BGTSP423	MDX-4-4210	Dow Corning	Silicone elastomer, bare edge assembly of bond chip design.
BGTSP424	MDX-4-4210	Dow Corning	Silicone elastomer, bare edge assembly of bond chip design.
BGTSP427	MDX-4-4210	Dow Corning	Silicone elastomer, bare edge assembly of bond chip design.
G42101	MDX-4-4210	Dow Corning	Silicone elastomer, bare edge assembly of grooved bond chip design.
PEM25A	PEM25	Huls	Silicone elastomer (MDX44210 like), bare edge assembly of bond chip design.
G42102	MDX-4-4210	Dow Corning	Silicone elastomer, bare edge assembly of grooved bond chip design (no UV Ozone).
F22186	A-2186	Factor II	Silicone elastomer (MDX44210 like), bare edge bond chip design (no UV Ozone).

TLS30A	LSR-30	Applied Silicone	Silicone elastomer (MDX44210 like), long TT devices in jar (no UV Ozone).
T4210A	MED-4210	NuSil Technology	Silicone elastomer (MDX44210 like), long TT devices in jar (no UV Ozone).
T4211A	MED-4211	NuSil Technology	Silicone elastomer (MDX44210 like), long TT devices in jar (no UV Ozone).
T3521A	CF2-3521	NuSil Technology	Fluorosilicone elastomer, long TT devices in jar (no UV Ozone).
T6210A	MED-6210	NuSil Technology	Optically clear silicone elastomer, long TT devices in jar (no UV Ozone).
T2620A	R-2620	NuSil Technology	Low viscosity impreg silicone, tan colored, long TT devices in jar (no UV Ozone).

Table 1: Test devices that have not yet failed saline immersion at 37°C under continuous 5 volt bias. Test results are summarized in **Table 2.**

Device ID	Material	Pair 1 Ω/□	Yr	Pair 2 Ω/□	Yr	Pair 3 Ω/□	Yr	Pair 4 Ω/□	Yr
D4210T	MED-4210	2.19E+18	1.5	6.00E+18	1.5	4.25E+18	1.5	6.10E+18	1.5
D6863W01	X-6863B	5.43E+18	5.3	2.40E+18	5.3	4.42E+18	5.3	6.25E+18	5.3
BGTSP681	X-6863	3.30E+15	5.9	1.61E+13	0.1	3.17E+15	5.9	5.70E+15	5.9
S6863W66	X-6863B	1.80E+18	6.0	1.64E+18	6.0	1.51E+18	6.0	1.53E+18	6.0
S6863W02	X-6863B	5.30E+18	5.6	1.69E+11	5.6	2.62E+18	5.6	5.80E+18	5.6
S8069W01	X-8069	6.95E+18	5.6	1.55E+13	5.6	4.71E+18	5.6	7.10E+18	5.6
BGTSP421	MDX-4-4210	4.11E+11	1.9	6.28E+16	7.4	6.63E+16	7.4	5.95E+16	7.4
BGTSP423	MDX-4-4210	1.54E+11	0.0	1.57E+12	1.3	8.29E+19	7.2	2.21E+19	7.2
BGTSP424	MDX-4-4210	3.51E+16	0.2	1.48E+18	6.9	7.33E+17	6.9	1.10E+17	6.9
BGTSP427	MDX-4-4210	1.73E+17	5.1	2.86E+17	5.1	1.96E+17	5.1	1.88E+17	5.1
G42101	MDX-4-4210	1.61E+08	2.3	7.10E+17	3.7	2.53E+17	3.7	5.85E+15	3.7
PEM25A	PEM25	1.06E+18	2.2	9.31E+17	2.2	*	*	4.48E+17	2.2
G42102	MDX-4-4210	2.70E+11	4.5	7.59E+09	0.5	2.16E+15	1.9	2.02E+19	1.9
F22186	A-2186	6.41E+15	2.4	4.52E+16	2.4	2.20E+17	2.4	6.55E+18	2.4
TLS30A	LSR-30	1.54E+17	1.4	1.02E+17	1.4	1.20E+17	1.4	8.80E+16	1.4
T4210A	MED-4210	2.36E+19	2.2	7.13E+19	2.2	7.63E+17	2.2	8.63E+19	2.2
T4211A	MED-4211	1.17E+13	0.0	3.73E+17	1.3	1.76E+18	1.3	1.35E+11	0.0
T3521A	CF2-3521	1.91E+15	1.4	4.00E+14	1.4	2.07E+14	1.4	2.59E+11	1.4
T6210A	MED-6210	9.13E+16	1.5	1.65E+17	1.5	1.02E+17	1.5	1.07E+17	1.5
T2620A	R-2620	3.60E+18	1.8	3.87E+19	1.8	3.10E+09	0.9	7.87E+18	1.8

Table 2: Equivalent surface resistivity for devices described in **Table 1.** Table is organized according to material. Note that all of these encapsulants are silicones. * indicates no data available.

Device ID	Material	Manufacturer	Description
BGTSP425	MDX-4-4210	Dow Corning	Silicone elastomer, bare edge assembly of bond chip design, 200C cure cycle.
G42103	MDX-4-4210	Dow Corning	Silicone elastomer, bare edge grooved bond chip design (no UV Ozone).
BGTSP426	MDX-4-4210	Dow Corning	Silicone elastomer, bare edge assembly of bond chip design. New clean room – first assembly.
CGTSP421	MDX-4-4210	Dow Corning	Silicone elastomer, coated edge assembly of bond chip design. H77 Epoxy overcoating all wires.
BGTSP611	R-6100	Dow Corning	Silicone elastomer, bare edge assembly of bond chip design.
BSP18401	Sylgard-184	Dow Corning	Silicone elastomer, bare edge assembly of bond chip design.
UGTSP490	H54U	Epoxy Technology	Unfilled epoxy, bare edge assembly of bond chip design.
AGTSG4	H54U	Epoxy Technology	Unfilled epoxy, coated edge assembly of bond chip design.
CGTSP77T	H77T	Epoxy Technology	Filled epoxy, coated edge assembly of bond chip design.
CGTSP377	377	Epoxy Technology	Unfilled epoxy, coated edge assembly of bond chip design.
BGTSP377	377	Epoxy Technology	Unfilled epoxy, bare edge assembly of bond chip design.
U2TSP490	H54U	Epoxy Technology	Unfilled epoxy, coated edge assembly of bond chip design.
BGTSP77T	H77T	Epoxy Technology	Filled epoxy, bare edge assembly of bond chip design.
LE301A	301	Epoxy Technology	Unfilled epoxy, bare edge assembly of bond chip design into long tube.

Table 3: Device descriptions for failed assemblies. Measurement data is shown in **Table 4**.

Device ID	Material	V03E04Ω/□	Yr	V05E06Ω/□	Yr	V07E08Ω/□	Yr	V09E10Ω/□	Yr
BGTSP425	MDX-4-4210	2.48E+12	6.6	4.10E+08	2.0	2.06E+07	3.5	1.17E+13	3.2
G42103	MDX-4-4210	2.68E+08	1.3	9.31E+06	1.3	4.38E+09	1.3	1.75E+07	1.3
BGTSP426	MDX-4-4210	4.03E+09	0.6	8.34E+12	0.6	1.49E+12	0.6	2.40E+13	0.4
CGTSP421	MDX-4-4210	8.41E+08	0.3	5.10E+09	0.3	1.93E+10	0.3	1.45E+11	0.4
BGTSP611	R-6100	5.41E+11	0.2	6.62E+08	0.2	2.36E+07	0.2	7.40E+08	0.1
BSP18401	Sylgard-184	1.72E+08	0.2	1.32E+07	0.2	1.65E+08	0.1	5.20E+07	0.1
UGTSP490	H54U	2.70E+06	0.2	3.45E+06	0.2	4.17E+06	0.2	5.00E+06	0.2
AGTSG4	H54U	1.90E+13	0.1	1.12E+13	0.1	1.50E+13	0.1	1.98E+12	0.1
CGTSP77T	H77T	7.22E+11	0.1	1.17E+12	0.1	9.00E+12	0.0	2.12E+12	0.0
CGTSP377	377	3.84E+08	0.1	3.62E+10	0.1	4.50E+12	0.1	2.75E+12	0.1
BGTSP377	377	3.51E+06	0.1	4.48E+07	0.1	9.58E+06	0.1	1.50E+10	0.1
U2TSP490	H54U	3.78E+10	0.0	8.86E+11	0.1	6.79E+07	0.1	1.34E+09	0.0
BGTSP77T	H77T	2.30E+11	0.0	6.21E+12	0.0	2.17E+11	0.1	1.18E+08	0.1
LE301A	301	4.51E+08	0.1	5.66E+07	0.1	6.13E+07	0.1	2.44E+08	0.1

Table 4: Data from failed devices described in**Table 3**. Devices were designated as failures when all electrode pairs exhibited surface resistivites lower than $1x10^{14}\Omega/\square$.

Discussion

These results are consistent with the chemistry that likely occurs at the interface. Carbon-Oxygen- Silicon bonds which would predominate at the interface between an epoxy or any other organic polymer are much less stable in the presence of water than are the Silicon-Oxygen-Silicon bonds which bond silicones to the surface [18]. Thus silicone chemistry should be preferred over organic chemistry for long term protection of exposed metals on a silicon dioxide surface. The fact that silicone elastomers are permeable to water vapor did not diminish the protective effect. Apparently the silicone bonds at a clean surface of silicon dioxide prevent condensation of water vapor and thus conductive paths do not readily form.

The results observed here are also consistent with the work of P.E.K Donaldson. [Review of Donaldson's work when paper collection is complete later this week]. The observed failures with silicone encapsulations are probably due to several factors. Some of the failures may be attributed to improper cleaning and handling during assembly as mentioned in the results section. More rigorous and automated processing could prevent such mishaps. Failures involving a single IDE pair on a Bond Chip, which has four such pairs, may have been due to local defects involving one or more of the 20μm spaces between interdigitated electrodes. The defect could have been caused by residual surface contamination, deposition of particulates prior to encapsulation, or a 20μm contaminant in the silicone that found it's way to the surface interface. Such failures were usually detected within a few days or months, but some failures did not appear until many years after encapsulation.

Localized failure involving one IDE under a silicone encapsulation layer did not necessarily propagate to adjacent IDEs. For example, Pair 2 on device BGTSP681 tested fine before saline immersion, but then failed within a few days after saline immersion. Adjacent IDEs, however, have survived at greater than $10^{15}\Omega/\square$ for over 5 years thus far. Device BGTSP423 illustrates progressive failure. Initially, Pair 1 exhibited low resistivity. After 15 months, Pair 2 also began showing low resistivity. However, Pairs 3 and 4 continue to exhibit high surface resistivity after more than 7 years.

Silicone as an Implantable Material

If silicones are to be used for encapsulation of implantable devices, it is important to understand the biocompatibility of the material. Silicones are by far the most studied of all classes of biomaterials. Commonly used as breast implants, penile implants, testicular implants, joint replacements, cerebrovascular shunts, heart valves, cardiac pacing lead insulation, indwelling catheter material, intraocular lenses, carriers for cochlear electrodes, etc., this class of materials is the most biocompatible, long lasting material yet developed. Currently, silicone breast implants are still considered reliable and safe by the American Society of Plastic Surgery [19]. The main problem with older implants appears to be contracture of the fibrous capsule causing extrusion of silicone gel and oil into the surrounding tissue. Gels and oils cause intense biological responses and can lead to generalized immunologic responses [20]. Current investigations indicate that it may be possible to prevent the typical fibrous encapsulation of silicone implants by coating the silicone with a hydrophilic layer of collagen or povidine [21, 22]. In a study of cochlear implant electrodes [23], MDX-4-4210 showed no evidence of degradation following implantation for 16 weeks in the scala tympani and muscles of cats. This finding may be particularly important since the cochlear fluids are similar to cerebrospinal fluids.

Also, there was only a mild reaction to the silicone resulting in a tight fibrous sheath which is commonly found with this material. Mechanical tests of implanted silicones have also been conducted in humans [24, 25].

Heart valve poppets (balls of silicone) implanted for 52 days in a human had a surface to core dynamic shear modulus ratio of 0.98 meaning the outer surface of the balls had become slightly softer than the inner core. After 8 years, the ratio was 0.83 indicating progressive softening of the silicone material. They found that diffusion of water occurred faster than the degradation process. Perhaps other molecules such as lipids were responsible for the mechanical changes.

The mechanical properties of the silicone insulation from pacemaker leads recovered at times ranging from 3 days to 11 years were studied [24]. Results showed that silicone tubing suffers gradual structural changes that are reflected in tests of swelling due to solvents (cross link density), and pull tests using the tensile strength at 200% elongation as a measure. Roggendorf et al [26] tested a variety of materials including RTV silicones, a medical grade silicone, polyamide, and polyester. Implants were left for one year in dogs prior to analysis. In general for silicones, tensile strength decreased, elongation increased, and the materials softened. Polyamide and polyester became brittle and exhibited crack crazing. They found that the stress-strain characteristic of the materials rather than hardness was the most sensitive to changes in mechanical properties. By Infrared Spectroscopy using Attenuated Total Reflectance, Roggendorf et al [26] also showed that silicones took up lipid materials which may be related to the changes in mechanical properties. Roggendorf et al [26] summarized their findings by stating that ``If `aging' is taken to include any irreversible change in a polymer after its manufacture, not one stable plastic or elastomer thoroughly tested under *in-vivo* conditions is known at this time.'' This literature increased our interest in testing the electrical properties of these materials, and comparing the mechanical degradation to electrical degradation. It also points out the need to be aggressive in testing with a variety of techniques to increase the probability that potential failure mechanisms are discovered.

Other aspects of the implant studies focus on the immune response and bacterial infection problem. The behavior of polyurethane, polyether/polyester copolymer, polypropylene oxide, and Silastic® tympanic membranes with Staphylococcus-aureus middle ear infections was studied [27]. Results showed that only the Silastic® implants were not degraded by the infection. Further, the fibrous capsule about the Silastic® was also not changed by the infection, and only rarely were macrophages observed between the capsule and the Silastic®.

Breast implant data, and studies of immune reactions to silicone indicate that under some circumstances, adverse reactions to silicone implants do occur, particularly when silicone oils or gels, or small fragments of silicones erode from implants [28-30]. Hunt et al [31] in a study of liver pathology caused by circulating silicone particulates from kidney dialysis tubing was able to clearly identify silicone particulates in giant cells and verified the composition by X-ray Energy Dispersive Spectroscopy.

Thus it appears that solid silicones implanted in locations protected from mechanical forces are relatively biocompatible. However, low molecular weight silicones and silicone particulates may provoke an immune response. Also, long term implantation in a biological system may cause changes in silicones that were not observed in our long term saline soak evaluations.

Conclusions and Future Work

Silicones are one class of materials that may be able to encapsulate implantable microelectronic devices for long term immersion in saline environments. Meticulous cleaning of the silicon dioxide surface is essential for successful encapsulation of implantable microelectronics. The method we have used may be more complicated that necessary for some facilities depending on the cleanliness of the devices at the end of fabrication but prior to encapsulation. It may also depend on the cleanliness of the facility in terms of particulate and organic contamination of the air. Local experimentation to determine an economical but reliable method for assembly of these devices may be warranted if the expense of meticulous cleaning becomes prohibitive. It is essential, however, that the surfaces of the integrated circuit being encapsulated consist of silicon dioxide rather than an organic monolayer of contamination. Otherwise, the silicone encapsulant will bond to the contamination rather than the surface of the silicon dioxide. If this happens, device failure is essentially guaranteed as soon as water vapor reaches the interfacial contamination and attacks the weak organic bonds and/or solvates the contaminants and begins supporting electrochemical reactions at the surface.

Silicones are one class of materials that may be able to encapsulate implantable microelectronic devices for long term immersion in saline environments. Now, it is important to determine long term effects of implantation in a mammalian system. Mammalian systems provide a rich organic environment containing acids, bases, enzymes, oils, fatty acids, etc. In addition, at least in low concentrations, there are a variety of organic solvents that may profoundly affect the long term survival of the insulating properties of silicone encapsulants. Effects of sterilization procedures should be evaluated. Also, while many pitfalls are associated with stress accelerated testing, it is important to test more devices under more severe conditions to sort the many different encapsulants that are available. Thus a high temperature soak test should be added to the low temperature testing to further evaluate candidate materials. While lifetime predictions would not be possible given the number of potential mechanisms involved with encapsulation failure, high temperature soak testing may uncover previously unrecognized failure mechanisms that can then be specifically tested using specifically developed tests.

Acknowledgements: Special thanks to Bill Heetderks and Terry Hambrecht of NIH without whom this ongoing work would not have been possible. Various aspects of the Insulating Biomaterials work was funded by NIH Contracts NINCDS-N01-NS-7-2399, NINCDS-N01-NS-0-2399, Contract NINCDS -NO1-NS-3-2301, NINDS-N01-NS-62350. I would also like to thank Dr. Mark S. Wrighton for helpful discussions on chemistry; Lloyd D. Clark and Ling Pei Kung for help with early work on instrumentation and device fabrication; Lisa P. Devaney and Cynthia M. Vanaria for fabrication and assembly of most of the test structures; Jeanne Fiore of Dow Corning Corporation for providing experimental silicone encapsualnts; and Jim Gillinger and Del Petraitis of Nusil Corporation for helpful discussions and suggestions on silicone materials for this project.

Literature Cited

[1] K. L. Drake, K. D. Wise, J. Farraye, D. J. Anderson, and S. L. Bement, "Performance of planar multisite microprobes in recording extracellular single unit intracortical activity," *IEEE Transactions on Biomedical Engineering*, vol. 35, pp. 719-732, 1988.

[2] D. J. Edell, J. N. Churchill, and I. M. Gourley, "Biocompatibility of a silicon based peripheral nerve electrode," *Biomat Med Dev Art Org*, vol. 10, pp. 103-122, 1982.

[3] D. J. Edell, V. M. McNeil, T. V. Vo, L. D. Clark, and W. K. Durfee, "Factors influencing the biocompatibility of insertable silicon microshafts in cerebral cortex.," *IEEE Transactions on Biomedical Engineering*, vol. 39, 1992.

[4] P. K. Campbell, R. A. Normann, K. W. Horch, and S. S. Stensaas, "A chronic intracortical electrode array: Preliminary results.," *J. BIomed. Mater. Res.: Applied Biomaterials*, vol. 23, pp. 245-259, 1989.

[5] J. F. Hetke, J. L. Lund, K. Najafi, K. D. Wise, and D. J. Anderson, "Silicon ribbon cables for chronically implantable microelectrode arrays," *IEEE Transactions on Biomedical Engineering*, vol. 41, pp. 314-321, 1994.

[6] G. T. A. Kovacs, C. W. Storment, and J. M. Rosen, "Regeneration microelectrode array for peripheral nerve recording and stimulation," *IEEE Transactions on Biomed. Eng.*, vol. 39, pp. 893-902, 1992.

[7] J.-U. Meyer, H. Deutel, E. Valderrama, E. Cabruja, P. Aebischer, G. Soldani, and P. Dario, "Perforated silicon dices with integrated nerve guidance channels

for interfacing peripheral nerves," presented at IEEE Micro Electro Mechanical Systems, 1995.

[8] K. Najafi, J. Ji, and K. D. Wise, "Scaling limitations of silicon multichannel recording probes," *IEEE Transactions on Biomed. Eng.*, vol. 37, pp. 1-11, 1990.

[9] J. Pine, "Cultured Neuron Probe," California Institute of Technology, Pasadena, NIH NINDS Contract Quarterly Reports N01-NS-3-2393, 1996.

[10] W. Rutten, H. vanWier, and J. Put, "Sensitivity and selectivity of intraneural stimulation using a silicon electrode array.," *IEEE Trans Biomed Eng*, vol. 38, pp. 192-198, 1991.

[11] K. D. Wise, J. B. Angell, and J. B. Starr, "An integrated circuit approach to extracellular microelectrodes," *IEEE Trans Biomed Eng*, vol. 17, pp. 238-247, 1970.

[12] R. DeIasi and J. Russell, "Aqueous Degradation of Polyimides," *J Appl Polym Sci*, vol. 15, pp. 2965-, 1971.

[13] J. Lentini and G. Severson, "Humidity induced failures in parylene coated hybrids.," *Circuits Manufacturing*, vol. May, pp. 56-57, 1984.

[14] D. J. Edell, "Insulating Biomaterials," MIT, Cambridge, Quarterly Report NIH-NO1-NS-3-2301, 1996.

[15] D. Edell, "Coatings for Protection of Integrated Circuits," NIH-NINDS, Bethesda, Contract N01-NS-7-2399, October 1, 1987- September 31, 1990 1987.

[16] D. J. Edell, "Development of a Chronic Neuroelectric Interface," in *Biomedical Engineering*. Davis: University of California, 1980.

[17] D. J. Edell, "A peripheral nerve information transducer for amputees: long-term multichannel recordings from rabbit peripheral nerves," *IEEE Trans. Biom. Eng.*, vol. 33, pp. 203-213, 1986.

[18] W. Noll, *Chemistry and Technology of Silicones*, 2nd ed. New York: Academic Press, 1968.

[19] N. I. Cruz, "Current ststus of silicone breast implants," *Bol. Assoc. Med. P. Rico - Agosto*, pp. 326-328, 1991.

[20] M. B. Habal, "The biologic basis for the clinical application of the silicones," *Arch. Surg*, vol. 119, pp. 843-848, 1984.

[21] F. R. Christ, D. A. Fencil, S. V. Gent, and P. M. Knight, "Evaluation of the chemical, optical and mechanical properties of elastomeric intraocular lens materials and their significance," *J. Cataract Refract. Surg.*, vol. 15, pp. 176-184, 1989.

[22] D. G. Wallace, J. Rosenblatt, and G. A. Ksander, "Tissue compatibility of collagen-silicone composites in a rat subcutaneous model," *Journal of Biomedical Materials Research*, vol. 26, pp. 1517-1534, 1992.

[23] R. K. Shepherd, R. L. Webb, G. M. Clark, B. C. Pyman, M. S. Hirshorn, M. T. Murray, and M. E. Houghton, "Implanted material tolerance studies for a multiple-channel cochlear prosthesis," *411*, pp. 71-81, 1984.

[24] B. Dolezel, L. Adamirova, P. Vondracek, and Z. Naprestek, "In vivo degradation of polymers. ii. changes of mechanical properties and cross-link density in silicone rubber pacemaker lead insulations during long-term implanation in the human body," *Biomaterials*, vol. 10, pp. 387-392, 1989.

[25] E. F. Cuddihy, J. Moacanin, and E. J. Roschke, "In vivo degradation of silicone rubber poppets in prosthetic heart valves," *J. Biomed. Mater. Res.*, vol. 10, pp. 471-481, 1976.

[26] E. Roggendorf, "The biostability of silicone rubbers, a polyamide and a polyester," *J. Biomed. Mater. Res.*, vol. 10, pp. 123-143, 1976.

[27] D. Bakker, C. A. v. Blitterswijk, S. C. Hesseling, W. T. Daems, W. Kuijpers, and J. J. Grote, "The behavior of alloplastic tympanic membranes in Staphylococcus aureus-induced middle ear infection. i. quantitative biocompatibility evaluation," *Journal of Biomedical Materials Research*, vol. 24, pp. 669-688, 1990.

[28] R. M. Goldblum, R. P. Pelley, A. A. O'Donell, D. Pyron, and J. P. Heggers, "Antibodies to silicone elastomers and reactions to ventriculoperitoneal shunts," *Lancet*, vol. 340, pp. 510-513, 1992.

[29] L. P. Endo, N. L. Edwards, S. Lomgley, L. C. Corman, and R. S. Panuch, "Silicone and rheumatic diseases," *Seminars in Arthritis and Rheumatism*, vol. 17, pp. 112-118, 1987.

[30] E. R. Bogoch, "Silicone synovitis," *Journal of Rheumatology*, vol. 14, pp. 1086-1088, 1987.

[31] J. Hunt, M. J. G. Farthing, L. R. I. Baker, P. R. Crocker, and D. A. Levison, "Silicone in the liver: possible late effects," *Gut*, vol. 30, pp. 239-242, 1989.